J Mater Sci (2011) 46:3046–3051
DOI 10.1007/s10853-010-5182-0

Influence of polymer infiltration and pyrolysis process on mechanical strength of polycarbosilane-derived silicon carbide ceramics

Takahiro Namazu · Tomohiro Ishikawa · Yoshio Hasegawa

Received: 17 August 2010 / Accepted: 9 December 2010 / Published online: 23 December 2010

Abstract In this article, strength evaluation of silicon carbide (Si–C) ceramics fabricated from polycarbosilane (PCS) precursor is described. Si–C ceramics was prepared by firing a green body made of the mixture of Si–C nanopowders and a PCS solution at 1,273 K in N_2 gas for an hour. To obtain dense Si–C, the solution was infiltrated into the produced body, and then it was fired again. The polymer infiltration and pyrolysis (PIP) process was conducted up to 12 cycles. Si–C ceramics was diced to be rectangle shape measuring 1.0 mm × 3.0 mm × 0.5 mm, and was subjected to the three-point bending test for measurement of the Young's modulus and bending strength. Si–C specimens fabricated through PIP processes less than 2 cycles showed non-linear force–displacement curves like a polymer, whereas those through the processes more than 3 cycles showed linear relations and fractured in a brittle manner. The Young's modulus of 12-cycles-PIPs specimen was found to be 56 GPa on average, which was approximately 22-fold of non-PIP specimen. The bending strength was also increased with an increase in the number of PIP process. The maximum value was found to be 157 MPa. The cause of the influence of PIP process on the mechanical characteristics is discussed using a PCS-derived Si–C model.

T. Namazu (✉) · T. Ishikawa
Department of Mechanical and Systems Engineering, Division of Mechanical Systems, University of Hyogo, 2167 Shosha, Himeji, Hyogo 671-2201, Japan
e-mail: namazu@eng.u-hyogo.ac.jp

Y. Hasegawa
R&D Division, ART KAGAKU Co., Ltd, 3135-20, Muramatsu, Tokai-mura, Naka-gun, Ibaraki 319-1112, Japan

Introduction

Power microelectromechanical systems (MEMS) device is one of the significant concerns in the aerospace and energy harvesting fields [1–7]. In operation of the device, temperature typically rises to several hundred degrees Celsius, so that the structural materials must possess good heat resistance and mechanical characteristics. In the MEMS field, silicon-related materials, such as single and poly crystal silicon (SCS and PCS), silicon oxide film, and silicon nitride film are commonly used as the structural materials because MEMS originated from semiconductor industry. As is well known, those materials are finely shaped to a micro or nanometer scale three-dimensional structure using semiconductor fabrication technologies. However, they do not have heat resistance enough for application to the structural material in power MEMS.

For the last decade, silicon carbide (Si–C), which is one of the heat resistant ceramics, attracts much attention as a structural material for power MEMS. Si–C is typically prepared by chemical vapor deposition (CVD) or sintering [8–15]. Si–C film prepared by CVD is useful for surface modification of a micro device because the material shows superior characteristics, such as small thermal expansion coefficient, less abrasion, high density, and chemical inertness. Si–C structure made by sintering has also good characteristics as does that by CVD. In the cases of CVD and sintering, however, fabricating three-dimensional arbitrary shape at the micro scale is very difficult because Si–C basically has excellent mechanical strength and chemical inertness. Several researchers have so far made many efforts to produce ceramics MEMS elements by using polymer precursor method [16–21]. In this method, a precursor polymer is firstly cast into a micro mold fabricated by UV-thick-photoresist lithography. Then the cast

polymer is pyrolyzed in an inert gas in order to convert into self-similar shaped ceramics. However, the polymer-derived ceramics elements are known to become porous, which provides the reliability of ceramics MEMS structures with a negative effect.

We have fabricated polymer-derived Si–C ceramics MEMS made from polycarbosilane (PCS) [22–24]. To make dense Si–C ceramics element, the polymer infiltration and pyrolysis (PIP) process was adopted. In this article, we focus on investigating the mechanical characteristics, such as Young's modulus and bending strength, by means of the three-point bending test. The influence of PIP process on those properties is discussed on the basis of a PCS-derived Si–C model.

Experimental procedure

Fabrication of Si–C ceramics

To fabricate Si–C ceramics, we used PCS as an organic precursor. To make Si–C with high ceramics yield, the use of ultrahigh molecular weight PCS prepared by fractional precipitation is effective. The organic structure made from PCS is converted to an inorganic structure through pyrolytic heat treatment at over 1,073 K [25]. In this case, the ceramics yield of 84% for PCS is theoretically obtained, and volume shrinkage rate is calculated to be approximately 1.8%. Firing at higher temperature is more effective for fabricating strong Si–C network.

As the first step for fabricating PCS-derived Si–C ceramics, the 40%-PCS toluene solution was mixed with Si–C nano-powder derived from PCS to make Si–C powder coated with PCS. The volume ratio of PCS to the powder was 1:10. PCS-coated Si–C powder containing stearic acid of 2 wt% was filled into a mold under a constant pressure of 80 MPa. Then, the green body was removed from the mold, and fired at 1,273 K in Ar gas. After firing, the Si–C body was obtained. Since the body had a lot of pores, it was immersed in a PCS solution to fill it into the pores by means of vacuum degassing. Then, firing at 1,273 K for an hour was performed again. The PIP process was conducted multiple cycles (up to 12 cycles) to improve its porosity. The Si–C body was mechanically cut by using a dicing saw to form rectangle-shaped structures measuring 1.0 mm × 3.0 mm × 0.5 mm, which were utilized as the specimens for the three-point bending test.

Figure 1 shows the relationship between the number of PIP process and porosity. Porosity was defined as a percentage of pore area to cross-section prepared by dicing cut. Porosity was decreased with an increase in the number of PIP process. For example, the porosity of Si–C ceramics after the first PIP process was approximately 25%, which

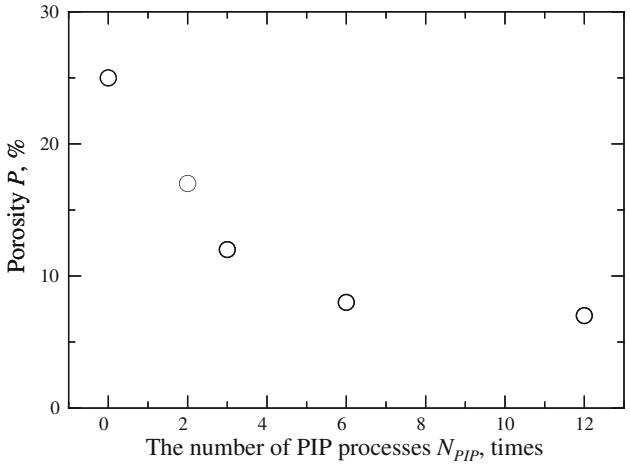

Fig. 1 Relationship between the number of PIP processes and porosity. Porosity is definitely decreased with an increase in the number of PIPs

decreased to 8% after 6-cycles-PIPs. Further PIP processes, however, did not bring drastic improvement. After 12-cycles-PIPs, the porosity was 7.5%, which is only 6.25% reduction from 6-cycles-PIPs specimen. This is because, in the case of low porosity region, filling a PCS solution into pores was difficult due to very small pore size or formation of closed pores.

Bending test

Figure 2 shows photographs of three-point bending tester for microscale Si–C ceramics specimen. The specially developed bending tester designed for miniature specimen consists of a piezoelectric actuator in an Al case for applying bending force, a load cell for bending force measurement, a laser displacement meter for specimen deflection measurement, loading and supporting jigs for realizing three-point bending deformation, and positioning stage for precisely setting a specimen between those jigs. The tester is able to apply bending force to a specimen in the horizontal direction to easily observe specimen deformation from its overhead with a CCD camera during bending. The load cell and laser displacement meter have a measurement resolution of 0.1 N and 10 nm, respectively. Loading and supporting jigs were made of cemented carbide to restrain elastic deformation of those jigs as small as possible. The distance between supporting points is 2.4 mm. The radius of curvature in supporting and loading jigs is 0.3 mm.

It is difficult to properly set a minute specimen between loading and supporting jigs because it is bent along the horizontal direction. As illustrated in Fig. 3, Si–C specimen is firstly settled on specimen holder, and then x-stage set under supporting jigs is moved toward loading jig until

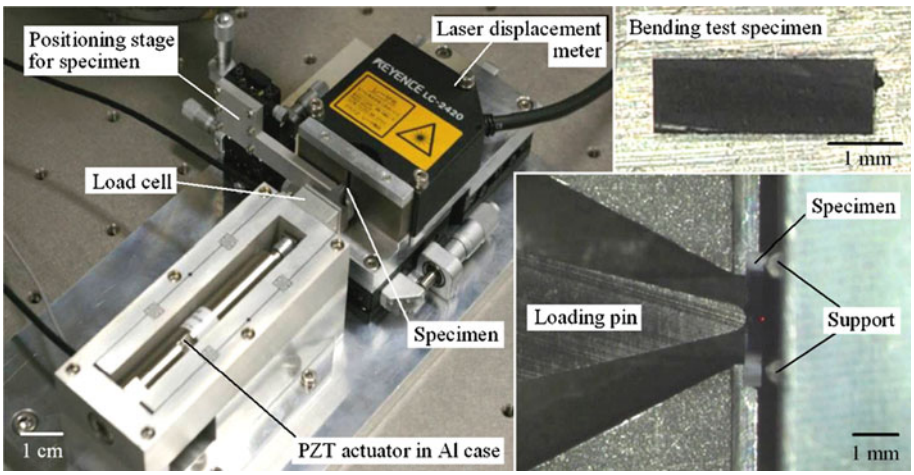

Fig. 2 Photographs of specially developed three-point bending tester for miniature Si–C ceramics specimen

the specimen contacts to both the jigs. After the specimen is held, the holder is removed, and then the three-point bending test is ready to start.

Results and discussions

Bending test result

Figure 4 shows representative bending force–deflection relations of Si–C specimens prepared through the PIP processes of 0, 3, 6, and 12 cycles. All the specimens were bent to failure at room temperature. Humidity was not controlled during the test. The loading speed was kept constant to be 0.167 μm/s. Non-PIP specimen shows non-linear force–displacement relation which slope is very small. The bending force hardly increases even when bending displacement increases until failure. No obvious yield point is seen. 2-cycles-PIPs specimen shows a similar trend as does non-PIP specimen. The maximum bending force is seen at the displacement of 1.5 μm, and then the force gradually drops to failure. At the beginning of bending test for 3-cycles-PIPs specimen, the force–displacement relation is linear. The slope is definitely larger than that of non- and 2-cycles-PIPs specimens. The bending force drastically drops at the deflection of 3.2 μm, but the force does not reach to 0 N. By virtue of rapid crack propagation into the specimen, the first fracture occurred, but the entire specimen did not fracture completely. After the first large fracture, probably lots of small fractures happened sequentially at the vicinity of the crack tip. 6- and 12-cycles-PIPs specimens show the same behavior that the force–displacement relation is almost linear until failure. At the deflection of 4.4 μm, bending force immediately drops to 0 N, indicating that brittle failure happened abruptly. From the bending test results described above, it is considered that "apparent" ductile–brittle deformation boundary would exist in Si–C ceramics produced through 2- or 3-cycles-PIPs.

Figure 5 shows the relationship between the number of PIP process and the Young's modulus of Si–C ceramics. The Young's modulus was calculated from the slope of force–displacement relation in the beginning of the test. The modulus of non-PIP specimen is found to be 2.5 GPa on average. This value is very low as with a polymer, which would be caused by low density and insufficiency

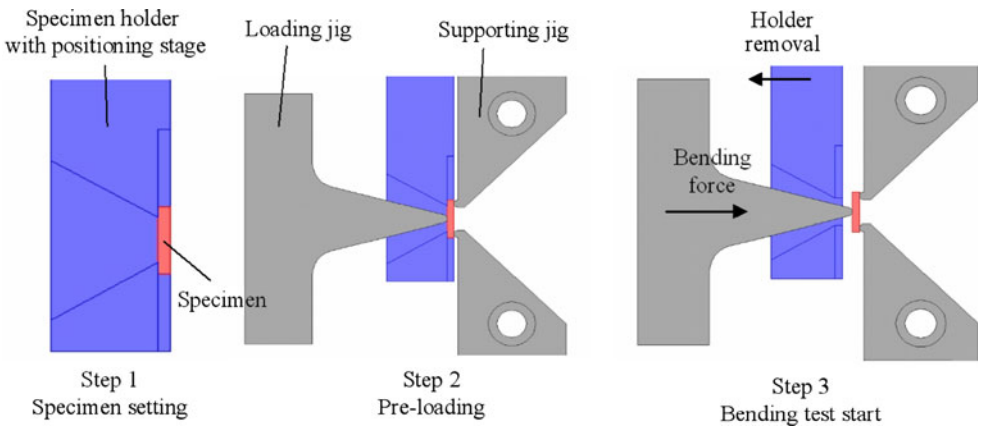

Fig. 3 Schematic of specimen setting between loading and supporting jigs

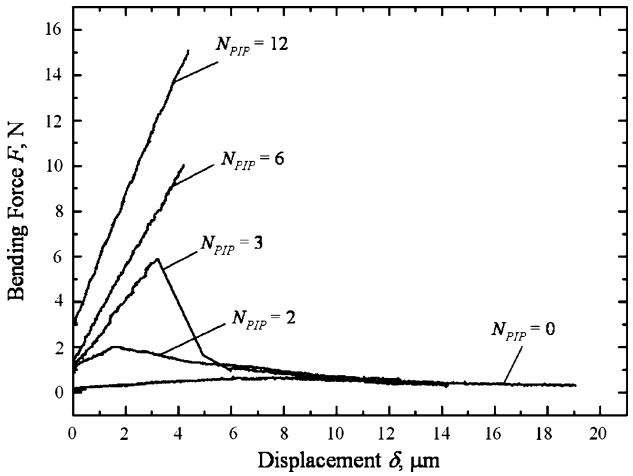

Fig. 4 Representative bending force–displacement relations of polymer-derived Si–C ceramics specimens. Apparent ductile–brittle transition was observed at the N_{PIP} between 2 and 3

sintering. With an increase in the number of PIP process to 3 cycles, the modulus remarkably increases to 45 GPa. This indicates that the specimen can rapidly harden by conducting a few PIP processes. After 3-cycles-PIPs processes, the increment in Young's modulus gradually decreases with increasing the number of PIP process. The mean value for 12-cycles-PIPs specimen is 56 GPa, approximately 22 times of that for non-PIP specimen. The maximum value of 68 GPa was obtained, which is about one-sixth of the Si–C bulk value [26, 27]. Compared with PCS-derived Si–C fibers, the value is about 0.36 times [28]. The difference would be caused by poor crystallinity and/or low density of the Si–C body. And also, in the PCS-derived Si–C body fired at 1,273 K, carbon-rich composition is typically obtained, and it might have given rise to low Young's modulus [29, 30].

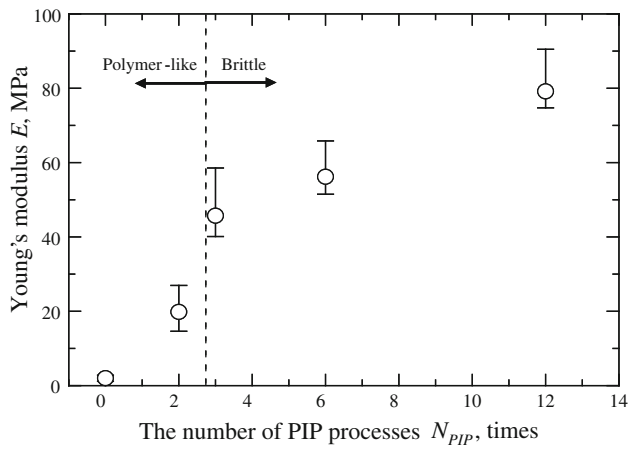

Fig. 5 Young's modulus vs. the number of PIP processes

Weibull statistics of bending strength

Figure 6 shows the Weibull plot of bending strength for Si–C ceramics. Total 56 specimens were subjected to the bending test. The strength data of all the specimens under respective PIP conditions were lined up on Weibull probability plotting paper, and could be approximated by respective straight lines. This indicates that 2-parameter Weibull distribution function is appropriate for the data fitting [31]. The slopes of respective lines are closely related to the variability of strength for each specimen, and tend towards vertical with an increase in the number of PIP process.

Figure 7 shows the relationships between the number of PIP process, scale, and shape parameters. The closed and open plots are indicative of the scale and shape parameters of Weibull, respectively. The scale parameter of non-PIP specimen is found to be about 9 MPa, which is quite lower than the bulk strength [32]. The parameter rapidly increases with increasing the number of PIP process as does the Young's modulus. After 6-cycles-PIPs, the parameter drastically increases to 140 MPa, which is approximately 15 times higher than that in non-PIP specimen. The strength increase is probably associated with a decrease in porosity. Multiple PIP processes can definitely reduce the size of pores that is thought to play a role as stress riser, and also can provide the formation of strong PCS-derived Si–C linkages between Si–C particles because of sintering time period accumulation. After 12-cycles-PIPs, however, the strength shows another 10% increase only from the strength of 6-cycles-PIPs specimen. This implies that, in low porosity region after several PIP processes, a change of porosity affecting strength was small. The maximum strength value obtained was 157 MPa, which is only 8.3%

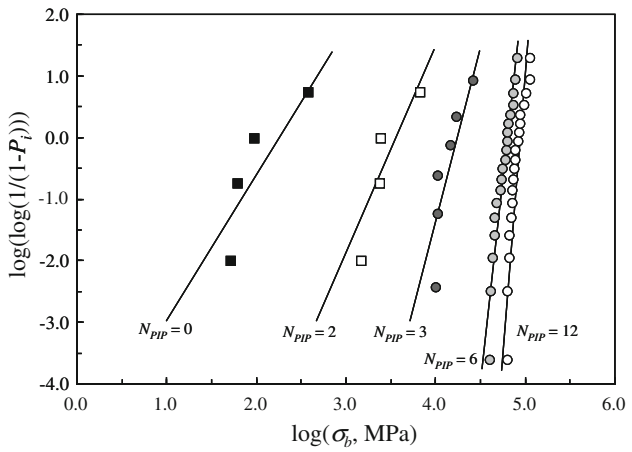

Fig. 6 Weibull plot of bending strength of polymer-derived Si–C ceramics specimens. Total 56 specimens were subjected to the three-point bending test. Two-parameter Weibull distribution function could be used to fit the strength data

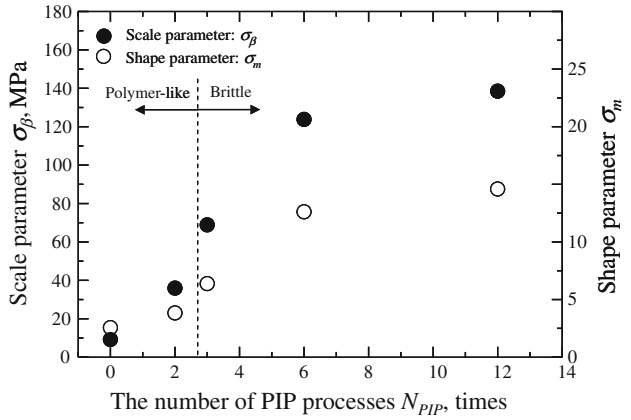

Fig. 7 Relationships between the number of PIP processes, scale and shape parameters of Weibull

of the strength of Si–C fiber [28]. On the other hand, the shape parameter of non-PIP specimen is calculated to be 2.6, which increases to 14 with increasing the number of PIP process to 12 cycles. Therefore, the number of PIP process has large influence on the improvement of specimen strength and its scatter.

Fracture mechanism

Figure 8a–c show scanning electron microscope (SEM) photographs of the fracture surface of Si–C ceramics produced through the PIP processes of 0, 6, and 12 cycles, respectively. In Fig. 8a, non-PIP specimen possesses irregular rough surface indicating that there are a lot of pores inside the body. The fracture surface shows a similar irregularity to side surface, so that fracture origin and river pattern indicating crack propagation direction cannot be found. Meanwhile, as shown in Fig. 8b, c, the specimen's side surface is relatively smooth, compared with non-PIP specimen. The surface flatness was brought about by conducting multiple PIP processes. These specimens have visible river pattern on their fracture surfaces. The river pattern starts from a specimen surface and proceeds to the inside. This indicates that the fracture origin would have existed at the vicinity of specimen surface where the maximum tensile stress generated during the bending test.

From the bending test results, the influence of PIP process on mechanical characteristics was clearly observed. The mechanism can be explained using the Si–C ceramics model before and after multiple PIP processes, as illustrated in Fig. 9. After the first PIP process illustrated in the left figure, PCS-derived Si–C nano-powders were coated once with a PCS solution, which was fired once at 1,273 K for an hour. Although the Si–C body was fired, it was weak. This is because, compared with that of Si–C particles, the rigidity of the coating layer is thought to be very low though the organic precursor was fully pyrolyzed. In addition, because PCS definitely shrunk during the firing, many voids were

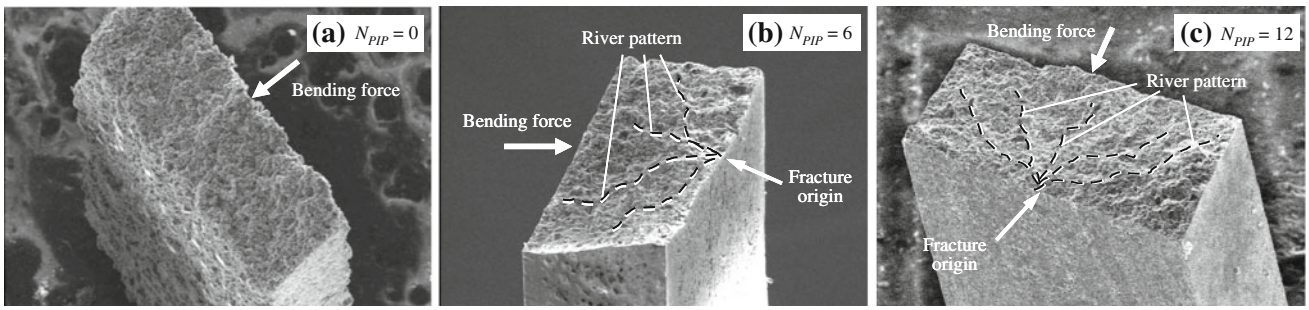

Fig. 8 SEM micrographs of fracture surface

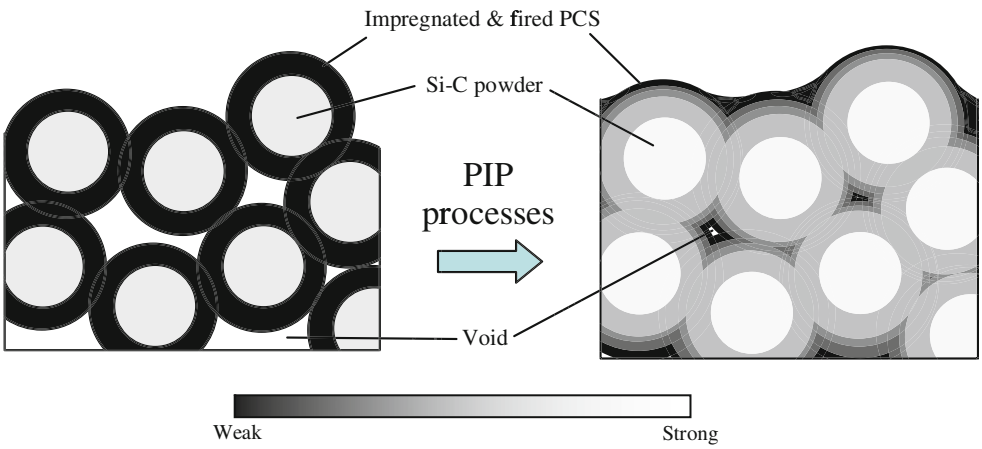

Fig. 9 Schematic diagram of PCS-derived Si–C ceramics specimens before and after multiple PIP processes

produced in the coating layer. One weakest PCS linkage between Si–C particles where the maximum tensile stress was produced was firstly broken by applying external force, and then other linkages around the failed link successively fractured one by one even when applied force was small. The successive brittle fractures of pyrolyzed linkages probably appeared as "apparent" ductility in the force–displacement relations. On the other hand, after several PIP processes, as shown in the right figure, the impregnated PCS was fired many times; consequently, many of unnecessary atoms included in the PCS vaporized, and the pyrolyzed PCS layer definitely toughened. By virtue of multiple impregnations and firings, the number of voids decreased and those sizes were reduced. Once a crack initiated, it probably propagated soon into strong Si–C body, and finally catastrophic failure of the entire body would have occurred. From those mechanisms described above, therefore, it is contemplated that the produced Si–C ceramics have strengthened mechanically with an increase in the number of PIP process.

In future, if porosity can be reduced a few % more by realizing further PIP processes, the mechanical characteristics would be better. In this study, although the reasonable model explaining the cause of the PIP effect on strength was proposed, the discussion on this should not be concluded until the structural analyses of fired PCS have been carried out.

Conclusion

We fabricated Si–C ceramics micro-elements derived from PCS precursor polymer, and evaluated their mechanical characteristics by means of three-point bending test. The produced Si–C body was immersed into a PCS solution, and then firing at 1,273 K was performed. This PIP process was carried out up to 12 cycles, in order to improve their poor porosity. Force–displacement relation of non-PIP specimen was non-linear, whereas that after 3-cycles-PIPs were almost linear until brittle failure. This indicated that apparent deformation characteristic was changed by conducting multiple PIP processes. The Young's modulus and strength of non-PIP specimen were 2.5 GPa and 9 MPa, respectively. After 12-cycles-PIPs, those values drastically increased to 68 GPa and 157 MPa. A large number of PIP process yielded PCS-derived Si–C ceramics having better mechanical characteristics.

References

1. Tanaka H (2004) J Inst Electr Eng Japan E 122(1):262
2. Peilo F, Pisano A, Fu K, Walther DC, Knobloch A, Martinez F, Senesky M, Maboudian R (2003) IEEJ Trans SM 123(9):326
3. Hara M, Tanaka S, Esashi M (2002) In: Proceedings of the 19th sensor symposium, p 507
4. Kang P, Tanaka S, Esashi M (2005) J Micromech Microeng 15:1076
5. Takahashi K (2004) Aeronaut Space Sci Japan 52(609):262
6. Teramoto S, Nagashima T (2004) Aeronaut Space Sci Japan 52(609):267
7. Song SJ (2004) Aeronaut Space Sci Japan 52(610):297
8. Liew L, Zhang W, Bright M, Linan A, Martin L, Rishi R (2001) Sens Actuators A 89:64
9. Goto T (2007) J Jpn Soc Powder Powder Metall 54(12):863
10. Shah SR, Raj R (2002) Acta Mater 50:4093
11. Taguchi T, Igawa N, Yamada R, Futakawa M, Jitsukawa S (2001) Ceram Eng Sci Proc 22(3):533
12. Oh JH, Choi DJ (2000) J Mater Sci Lett 19(22):2043
13. Beyer S (1999) Development and testing of C/SiC components for liquid rocket propulsion applications. Pap Am Inst Aeronaut Astronaut, p 12
14. Niu J, Kijima K, Nakahira A, Tanaka K (1999) Proc Ceram Soc Japan 1999:289
15. Chen L, Goto T, Hirai T (1996) J Mater Sci 31(3):679. doi: 10.1007/BF00367885
16. Liew L-A, Zhang W, An L, Shah S, Luo R, Liu Y, Cross T, Dunn ML, Bright V, Daily JW, Raj R, Anseth K (2001) Am Ceram Soc Bull 50(5):25
17. Nagaiah NR, Kapat JS, An L, Chow L (2006) J Phys 34:458
18. Kong JS, Frangopol DM, Raulli M, Maute K, Saravanan RA, Liew L-A, Raj R (2004) Sens Actuators A 116:336
19. Lee D-H, Park K-H, Hong L-Y, Kim D-P (2007) Sens Actuators A 135:895
20. Liew L-A, Saravanan RA, Bright VM, Dunn ML, Daily JW, Raj R (2003) Sens Actuators A 103:171
21. Liu Y, Liew L-A, Luo R, An L, Dunn ML, Bright VM, Daily JW, Raj R (2002) Sens Actuators A 95:143
22. Hasegawa Y, Okamura K (1983) J Mater Sci 18:3633. doi: 10.1007/BF00540736
23. Hasegawa Y, Okamura K (1986) J Mater Sci 21:321. doi:10.1007/BF01144739
24. Ishikawa T, Namazu T, Yoshiki K, Inoue S, Hasegawa Y (2010) In: Proceedings of the Microelectromechanical Systems, MEMS 2010, p 416
25. Hasegawa Y (2006) In: Proceedings of the 55th polymer conf: 3003–3004
26. Suyama S, Itoh Y (2006) Rev TOSHIBA 61(6):72
27. Zhang H, Yan Y, Huang Z, Liu X, Jiang D (2009) J Am Ceram Soc 92(7):1559
28. Day RJ, Piddock V, Taylor R, Young RJ, Zakikhani M (1989) J Mater Sci 24:2898. doi:10.1007/BF02385644
29. Tuinstra F, Koenig JL (1970) J Compos Mater 4:492
30. Sasaki Y, Nishina Y, Sato M, Okamura K (1986) Yogyo-Kyokai-Shi 94(8):897
31. Namazu T, Isono Y, Tanaka T (2000) J Microelectromech Syst 9(4):450
32. Hurtado AM, Alkan Z (1993) Ceram Int 19(5):327